Astronomy and Space Science: Open Access
Received: Apr 17, 2018, Accepted: May11, 2018, Published: May 15, 2018
Astron Space Sci, Volume 4, Issue 1
http://crescopublications.org/pdf/ASSOA/ASSOA-4-012.pdf
Article Number: ASSOA-4-012

Research Article | ISSN: 2472-9620 | Open Access

Effect of Kappa Distribution Function on Electrostatic Ion Cyclotron Waves in Multi-Ions Magnetospheric Plasma by Particle Aspect Approaches

Vibhooti Khaira* **and G. Ahirwar**

School of Studies in Physics, Vikram University, Ujjain (M.P.) 456010, India

***Corresponding author:** Vibhooti Khaira, School of Studies in Physics, Vikram University, Ujjain (M.P.) 456010, India, E-mail: khaira.vibhuti29@gmail.com

Citation: Vibhooti Khaira and G. Ahirwar (2018) Effect of Kappa Distribution Function on Electrostatic Ion Cyclotron Waves in Multi-Ions Magnetospheric Plasma by Particle Aspect Approaches. Astron Space Sci 4: 012.

Abstract

In this paper, we have investigated of electrostatic ion cyclotron waves in multi-ions plasma (H^+, He^+ and O^+) using particle aspect analysis. The kappa distribution function, dispersion relation, growth rate have been derived for EIC waves in multi-ions plasma. The whole plasma is considered to consist of resonant and non-resonant particles. It is assumed that the resonant particles participate in energy exchange while the non-resonant particles support the oscillatory motion of the wave. The wave is assumed to propagate obliquely to the static magnetic field. It is observed that the effect of kappa distribution function in multi-ions (H^+, He^+ and O^+) of EIC waves is to enhance the growth rate. The results are interpreted for the space plasma parameters appropriate to the auroral acceleration region around on earth's magnetosphere. The advantages of present approach and study are to its suitability for dealing and determining the effect of kappa distribution function on EIC waves.

Keywords: Electrostatic ion-cyclotron wave; Particle aspect approach; Auroral acceleration region; Kappa distribution function; Multi-component plasma.

1. Introduction

The Electrostatic ion cyclotron waves were first discovered by D` Angelo and Motley Drummond and Rosenbluth in 1962 [1]. These waves are normal mode of magnetized plasma. It is propagated almost perpendicularly to the magnetic field with a small, but finite parallel wave number $K_{||}$ so that electrons can maintain Boltzmann distribution by moving along the magnetic field, thus the ratio of parallel to perpendicular wave number is less than one. These waves are very narrowing banded and consequently turn out to be highly coherent over several oscillation periods. The excitation mechanism of these waves is the instabilities caused by electron currents, ion beams, loss-cone distribution and kappa distribution of energetic ions.

Particle velocity distribution functions in space plasmas often show non maxwellian super thermal tails decreasing as a power law of the velocity. Such distributions are well fitted by the so-called kappa distribution. The presence of such distributions in different space plasma suggests a universal mechanism for the creation of such super thermal tails. The super thermal particles have impotent consequences concerning the acceleration and the temperature that are well evidenced by the particle aspect approach where no closures require the distributions to be nearly maxwellian.

The well knows maxwellian and kappa distributions differ substantially in the high energy tail region. The drop towards zero is much more abrupt for a maxwellian distribution when compared to that of kappa distribution with a low spectral index k. Such conditions occur in space and other magnetospheric plasma and kappa distribution have been used to analysis and interpret spacecraft data in the earth's magnetospheric plasma sheet [2, 3] the solar wind [4, 5] Jupiter [6] and Saturn [7]. Studies of Pc1-5 waves have been undertaken near the high latitude Davis Antarctic station using a small network of magnetometers located in a square arrangement of side 120- 150km. Direction of arrival determinations on daytime quasi- structured and unstructured Pc1-2 emissions show they are associated with sources on closed field lines in the outer magnetosphere. This boundary region just inside the magnetopause may also be the origin of a pronoun Pc1-2 band, possibly a consequence of electrostatic ion cyclotron wave (ESIC) generation resulting from ion injection into the magnetosphere from the dayside cleft. It has also been shown that these waves may propagate over short distances (< 500 km) but are not propagated in the ionospheric F2 region waveguide.

The advantages of present approach and study is to its suitability for dealing and determining the effect of general loss cone distribution with kappa distribution on ESIC waves in multi-ions plasma i.e. H^+, He^+ and O^+ and determines the properties of the medium (plasma) in magnetosphere. The linear theory of plasma instabilities has been thoroughly studied in the past by several authors [8-11]. Electrostatic ion-cyclotron waves generated in the equatorial region of earth's magnetosphere as left-handed circularly (LHC) polarized waves propagate field line guided towards the ionosphere [12].

The main aim of this study is to investigate the generation of ESIC waves in multi-ions plasma i.e. H^+, He^+, O^+ and see the effect of kappa distribution in magnetospheric plasma. Present study is made sequentially to study the growth rate and resonant energies of ESIC waves with multi component plasma and loss- cone distribution function with kappa distribution. This study can help to understand the transport of plasma in the magnetosphere and electrodynamics of plasma sheet boundary layer region. Satellites dedicated to the study of the Earth's magnetosphere, such as Cluster Escoubet [13], the Geomagnetic Tail Lobe (GEOTAIL) Nishida [14], Double Star, Liu [15] or the Time History of Events and Macro scale Interactions during Sub storms (THEMIS) Angelopoulos [16]. These all satellites provided us very useful data which can help to make a better understanding about magnetosphere, earth environment and related mysteries.

2. Basic Assumption

The trajectories of particles are then evaluated within the framework of linear theory.

$K_\Pi E, k = (k_\perp, 0, k_\Pi)$, $E = (E_x, 0, E_z)$

With

$$E_x(r,t) = E_1 \cos(k_\perp x + k_\Pi z - \omega t),$$
$$E_z(r,t) = kE_1 \cos(k_\perp x + k_\Pi z - \omega t)$$

and

$$k = (\frac{k_\Pi}{k_\perp}) < 1$$

where

$$\phi = k_\perp x + k_\Pi z - \omega t$$

The amplitude E_1 is slowly varying function of t i.e $\frac{1}{E_1}(\frac{dE_1}{dt}) << \omega$

Here, k_{II} and $k_{\perp}$are the components of the wave vector along and across the magnetic field, respectively and ω represent the wave frequency.

2.1 Velocities of the Particle:

The trajectories of particles are evaluated within the framework of linear theory. The equation of motion of a particle is given by,

$$m(\frac{dv}{dt}) = q[E + (\frac{1}{c})v \times B_0] \quad (1)$$

If E is considered to be a small perturbation i.e. $E=E_0+E_1$, velocity v can be expressed in terms of unperturbed velocity V and perturbed velocity u.

Then the trajectories of the free gyration are obtained as;

$$\begin{aligned} X(t) &= \frac{V_{\perp}}{\Omega_{\alpha}}[\sin(\theta - \Omega_{\alpha}t) - \sin\theta] + Y_{0,} \\ Y(t) &= \frac{V_{\perp}}{\Omega_{\alpha}}[\cos(\theta - \Omega_{\alpha}t) - \cos\theta] + Y_{0,} \\ Z(t) &= V_{\Pi}t + Z_{0,} \end{aligned} \quad (2)$$

The perturbed velocity u is determined by;

$$\begin{aligned} \frac{du_{\perp}}{dt} + i\Omega_{\alpha}u_{\perp} &= \frac{qk_{II}E_1}{k_{\perp}m}\sum_{-\infty}^{+\infty} J_1(\mu)\cos(A_{\lambda}t + \psi_{\lambda}{}^0) \\ \frac{du_{\Pi}}{dt} &= \frac{qE_1}{m}\sum_{-\infty}^{+\infty} J_1(\mu)\cos(A_{\lambda}t + \psi_{\lambda}{}^0) \end{aligned} \quad (3)$$

Where $u_{\perp} = u_x + iu_y$ represents the perturbed velocity in transverse direction and $u_{\parallel}$represents the velocity in parallel direction.

The resonance criteria are given by;

$$A_{\lambda}(V_{\Pi} = V_r) = k_{II}V_{II} - \omega + \lambda\Omega_{\alpha} = 0; \lambda = \pm 1, \pm 2, \pm 3, \ldots\ldots\ldots\ldots$$

Here, V_r is the resonance velocity of the particles.

The oscillatory solution of u (t) is given by;

$$\begin{aligned} u_x(\rho.t) &= -\frac{qE_1}{m}\sum_{-\infty}^{+\infty} J_n(\mu) \times \left[\frac{A_{\lambda}}{A_{\lambda} - \Omega^2{}_{\alpha}} \sin\chi_{nl} - \frac{\delta}{2A_{n+1}}\sin(\chi_{nl} - A_{n+1}t) - \frac{\delta}{2A_{n-1}}\sin(\chi_{nl} - A_{n-1}t) \right] \\ u_y(\rho.t) &= \frac{qE_1}{m}\sum_{-\infty}^{+\infty} J_n(\mu)\sum_{-\infty}^{+\infty} J_{\lambda}(\mu) \times \left[\frac{A_{\lambda}}{A^2{}_{\lambda} - \Omega^2{}_{\alpha}}\cos\chi_{nl} - \frac{\delta}{2A_{n+1}}\cos(\chi_{nl} - A_{\lambda+1}t) - \frac{\delta}{2A_{\lambda-1}}\sin(\chi_{nl} - A_{\lambda-1}t) \right] \\ u_z(\rho.t) &= \frac{qk_{II}E_1}{k_{\perp}m}\sum_{-\infty}^{+\infty} J_n(\mu)\sum_{-\infty}^{+\infty} J_{\lambda}(\mu) \times \frac{1}{A_{\lambda}}\left[\sin\chi_{nl} - \delta\sin(\chi_{nl} - A_{n+1}t) \right] \end{aligned} \quad (4)$$

Here

$$\chi_{nl} = k.r - \omega t + (n - \lambda)(\Omega_{\alpha}t - \theta)$$

δ =0 for non-resonant particles and δ =1for resonant particles.

2.2 Distribution Function:

To determine the dispersion relation and growth rate, we consider bi-Maxwellian plasma as,

$$f_o(y, V) = N_o f_{\perp}(V_{\perp}) f_{\Pi}(V_{\Pi}) \quad (5)$$

We consider a general loss-cone distribution function for $f_{\perp}(V_{\perp})$ as

$$f_{\perp}(V_{\perp}) = \left[\frac{V^{2J}{}_{\perp}}{\pi V_{T\perp}{}^{2(J+1)}} \right] \exp\left(-\frac{V^2{}_{\perp}}{V_{T\perp}{}^2} \right) \quad (6)$$

And $f_{\parallel}(V_{\parallel})$which is defined by the drifting Maxwellian as

$$f_{II}(V_{II}) = \left[\frac{V^{2J}{}_{II}}{\sqrt{\pi} V_{II\perp}{}^{2(J+1)}} \right] \exp\left(-\frac{V^2{}_{II}}{V_{TII}{}^2} \right) \quad (7)$$

Here using the value of $V^2{}_{T\perp} = (J+1)^{-1}\frac{2T_\perp}{m}$ and $V^2{}_{TII} = \frac{2T_{II}}{m}$ for plasma and the bi-lorentzian, which reduces to the anisotropic bi-maxwellian distribution when the spectral index k tends to infinity is given by,

$$F = \frac{1}{\sqrt[3]{\pi}} \frac{\Gamma(\kappa + J + 1)}{\sqrt[3]{\kappa}\Gamma\kappa - 1/2 V^2{}_{T\perp} V^2{}_{TII}} [1 + \frac{V^2{}_{T\perp}}{KV^2{}_{T\perp}} + \frac{V^2{}_{TII}}{KV^2{}_{TII}}]^{-(\kappa+J+1)} \quad (8)$$

In equation (8) $V^2{}_{T\perp}$ and $V^2{}_{TII}$ are related to the mass m and the temperatures $T_\perp$ and T_{II} respectively parallel and perpendicular to the magnetic field by,

$$V^2{}_{T\perp} = (J+1)^{-1}[\frac{\kappa - 3/2}{\kappa}\frac{2KT_\perp}{m}] \quad (9)$$

$$V^2{}_{TII} = [\frac{\kappa - 3/2}{\kappa}\frac{2KT_{II}}{m}] \quad (10)$$

The quasi-neutrality condition yields to the equation:

$$n_e = n_{H^+} + n_{He^+} + n_{O^+}$$

Thus we evaluate the density perturbation associated with the particle velocity as:

$$\frac{dn_1}{dt} = -F_{H^+}(V)(\nabla.u)_{H^+} + (-F_{He^+}(V)(\nabla.u)_{He^+} + (-F_{O^+}(V)(\nabla.u)_{O^+} \quad (11)$$

The integration w.r.to t from equation (8) we get the solution for perturbed density as

$$n_1(r,t) = -\frac{qE_1F(V_\alpha)}{m_\alpha k^2{}_\perp} k_{II}{}^2 \sum_{-\infty}^{+\infty} J_\lambda(\mu)J_n(\mu) \times [\frac{k_\perp}{A^2{}_\lambda - \Omega^2{}_\alpha} + \frac{k_{II}{}^2 K_\perp}{k^2{}_\perp A^2{}_\lambda}] \sin\chi_{nl}$$

And

$$n_1(r,t) = \frac{qE_1F(V_{H^+})}{m_{H^+}k_\perp{}^2} k_{II}{}^2 K_\perp \sum_{\lambda,n=-\infty}^{+\infty} J_\lambda(\mu)J_n(\mu)\frac{1}{A^2{}_{\lambda H^+}} \{\sin(\chi_{n\lambda} - \sin(\chi_{n\lambda} - A_{\lambda H^+}t) - A_{\lambda H^+}t\cos(\chi_{n\lambda} - A_{\lambda H^+}t)\} +$$

$$\frac{qE_1F(V_{He^+\alpha})}{m_{He^+}k_\perp{}^2} k_{II}{}^2 K_\perp \sum_{\lambda,n=-\infty}^{+\infty} J_\lambda(\mu)J_n(\mu)\frac{1}{A^2{}_{\lambda He^+}} \{\sin(\chi_{n\lambda} - \sin(\chi_{n\lambda} - A_{\lambda He^+}t) - A_{\lambda He^+}t\cos(\chi_{n\lambda} - A_{\lambda He^+}t)\} +$$

$$\frac{qE_1F(V_{O^+})}{m_{O^+}k^2{}_\perp} k_{II}{}^2 K_\perp \sum_{\lambda,n=-\infty}^{+\infty} J_\lambda(\mu)J_n(\mu)\frac{1}{A^2{}_{\lambda O^+}} \{\sin(\chi_{n\lambda} - \sin(\chi_{n\lambda} - A_{\lambda O^+}t) - A_{\lambda O^+}t\cos(\chi_{n\lambda} - A_{\lambda O^+}t)\} \quad (12)$$

3. Dispersion Relation

We consider the cold plasma dispersion relation for the ESIC wave as;

$$n_{\alpha,e} = \mu\int dvF(v)\frac{eE_1K_\perp}{m_{\alpha,e}}\sum_{n\lambda}\left\{J_\lambda(\mu)J_n(\mu)\times[\frac{K_\perp}{A^2{}_\lambda - \Omega^2{}_\alpha} + \frac{k_{II}{}^2}{k^2{}_\perp A^2{}_\lambda}]\sin\chi_{nl}\right\} \quad (13)$$

Where $n_{\alpha,e}$ is integrated density and

$$\mu = \frac{K_\perp V_\perp}{\Omega_{\alpha,e}}, A = K_{II}V_{II} - \omega + n\Omega_{i,e}, \chi_{n\lambda} = k.r - \omega t + (n-l)(\Omega_\alpha l - \theta)$$

Using the expression, then the dispersion relation EIC waves in multi-component plasma is given by

$$n_e = (\frac{1}{k_\perp d^2{}_{IIe}})\frac{E_1}{4\pi e}\sin(kr - \omega t)$$

And $$n_\alpha = -\frac{k_{II}{}^2\omega^2{}_{p\alpha}1}{(\omega - \lambda\Omega_\alpha)k_\perp}\left\langle 1 - \frac{k^2{}_\perp\rho^2{}_\alpha}{2}(\frac{2\kappa - 3}{\kappa})\right\rangle\frac{E_1}{4\pi e}\sin(kr - \omega t)$$

Where $\alpha = H^+, He^+, O^+ and \omega^2{}_{p\alpha} = \frac{4\pi N_\alpha e^2}{m_\alpha}$ is the plasma frequency for multi-ions and N_α is the multi-ions plasma density.

Debye length (d^2_{IIe}) is given by

$$d^2_{IIe} = \frac{T_{IIe}}{m_e \omega^2_{pe}}$$

Using the Poisson's equation

$$\nabla . E = 4\pi e(n_\alpha - n_{e)} \tag{14}$$

The perturbed ion and electron density ni and ne the dispersion relation is obtain as

$$\omega = \Omega_\alpha + [\omega^2_{p\alpha} \left\langle 1 - \frac{k^2_\perp \rho^2_\alpha}{2}(\frac{2\kappa - 3}{\kappa}) \right\rangle (\frac{1}{\frac{k_\perp + k_{II}}{k_{II}^2 k_\perp} + \frac{k^2_\perp}{k_{II}^2}(\frac{1}{k^2_\perp d^2_{IIe}})})] \tag{15}$$

4. Wave Energy and Growth Rate

The wave energy W_w per unit wavelength is the sum of the pure field energy. The total energy per unit wavelength is given as

$$W_w = \frac{\lambda B^2}{8\pi} + W_e + W_{r\alpha}$$

Where $$W_e = \frac{\lambda E^2}{8\pi} + \frac{\lambda E^2}{16\pi}(\frac{1}{k_\perp d^2_{IIe}})$$

$$W_{r\alpha} = \sum_\alpha (W_{r\alpha\perp} + W_{r\alpha II})$$

and $$W_{r\perp} = \int_0^\lambda dz \int_0^\infty V_{\perp\alpha} dV_{\perp\alpha} \int_0^{2\theta} d\theta \int_{v_r - \Delta r}^{v_r + \Delta r} dV_{\Pi\alpha} \frac{m}{2}[(N + n_{1\alpha})(V_{\perp\alpha} + u_{\perp\alpha})^2 - N V_{\perp\alpha}{}^2] \tag{16}$$

$$W_{rII} = \int_0^\lambda dz \int_0^\infty V_{II\alpha} dV_{II\alpha} \int_0^{2\theta} d\theta \int_{v_r - \Delta r}^{v_r + \Delta r} dV_{\Pi\alpha} \frac{m}{2}[(N + n_{1\alpha})(V_{II\alpha} + u_{II\alpha})^2 - N V_{II\alpha}{}^2]$$

4.1 Perpendicular Resonant Energy

$$W_{r\perp\alpha} = (\frac{\lambda E^2}{8\pi})(\frac{\omega_{p\alpha}{}^2}{\Omega_\alpha{}^2})(\frac{\omega}{k_{II} V_{th\alpha}}) \frac{\Omega_\alpha t}{\sqrt{2\pi}} \exp\left\{ -\frac{1}{2}(\frac{\omega}{k_{II} V_{th\alpha}})^2 (1 - \frac{\lambda\Omega_\alpha}{\omega})^2 \right\} \times \frac{1}{2} \left\langle 1 - \frac{k^2_\perp \rho^2_\alpha}{2}(\frac{2\kappa - 3}{\kappa}) \right\rangle$$

$$\left[1 - (\frac{R(\frac{\lambda\Omega_\alpha}{\omega} - 1)}{\frac{\lambda\Omega_\alpha}{\omega}}) \frac{T_{\perp\alpha}}{T_{II\alpha}} \right] \tag{17}$$

4.2 Parallel Resonant Energy

$$W_{rII\alpha} = (\frac{\lambda E^2}{8\pi})(\frac{\omega_{p\alpha}{}^2}{\Omega_\alpha{}^2})(\frac{\omega}{k_{II} V_{th\alpha}}) \frac{\Omega_\alpha t}{\sqrt{2\pi}} \exp\left\{ -\frac{1}{2}(\frac{\omega}{k_{II} V_{th\alpha}})^2 (1 - \frac{\lambda\Omega_\alpha}{\omega})^2 \right\} \times \frac{1}{2} \left\langle 1 - \frac{k^2_\perp \rho^2_\alpha}{2}(\frac{2\kappa - 3}{\kappa}) \right\rangle$$

$$\left[(\frac{\lambda\Omega_\alpha}{\omega} - 1) (\frac{\omega}{\frac{\lambda\Omega_\alpha}{\omega}}) \frac{T_{\perp\alpha}}{T_{II\alpha}} \right] \tag{18}$$

Where

$$R = \frac{1 - \frac{1}{2}\frac{k^2_\perp \rho^2_\alpha}{2}(\frac{2\kappa - 3}{\kappa})}{1 - \frac{k^2_\perp \rho^2_\alpha}{2}(\frac{2\kappa - 3}{\kappa})}$$ and $\alpha = H^+, He^+, O^+$

4.3 Growth Rate

Using the law of conservation of energy the growth rate is obtained as

$$\frac{\gamma}{\omega}=\sqrt{\frac{\pi}{2}}\left(\frac{\omega}{k_{II}V_{th\alpha}}\right)\left(1-\frac{\lambda\Omega_{\alpha}}{\omega}\right)^{2}\exp\left\{-\frac{1}{2}\left(\frac{\omega}{k_{II}V_{th\alpha}}\right)^{2}\left(1-\frac{\lambda\Omega_{\alpha}}{\omega}\right)^{2}\right\}\times\left[\frac{R\left(\frac{\lambda\Omega_{\alpha}}{\omega}-1\right)\frac{T_{\perp\alpha}}{T_{II\alpha}}-1}{\frac{\lambda\Omega_{\alpha}}{\omega}}\right] \tag{19}$$

5. Results and Discussion

In the present analysis the expressions for the dispersion relation, resonant energies and growth rate are derived in the presence of kappa distribution of plasma ions. The following parameters relevant to the auroral acceleration region [17 - 20] are used to evaluate the dispersion relation, resonant energies and growth rate.

$B_o = 4300nT\ at\ 1.4R_E, K_\perp \approx 2.5\times10^{-3}m^{-1},, \omega_{pH}^2 = 1.552\times10^{9}sec^{-2},$

$\omega_{pHe}^2 = .216\times10^{8}sec^{-2}, \omega_{pO}^2 = .05\times10^{8}sec^{-2}$

$\Omega_H = 412sec^{-2}, \Omega_{He} = 103sec^{-2}, \Omega_O = 26sec^{-2}, \frac{T_\perp}{T_\parallel} = 50, k_BT_\parallel = 5eV.$

And A=$\frac{T_{\perp\alpha}}{T_{\parallel\alpha}}$ for multi-ions, here α=H^+, He^+, O^+

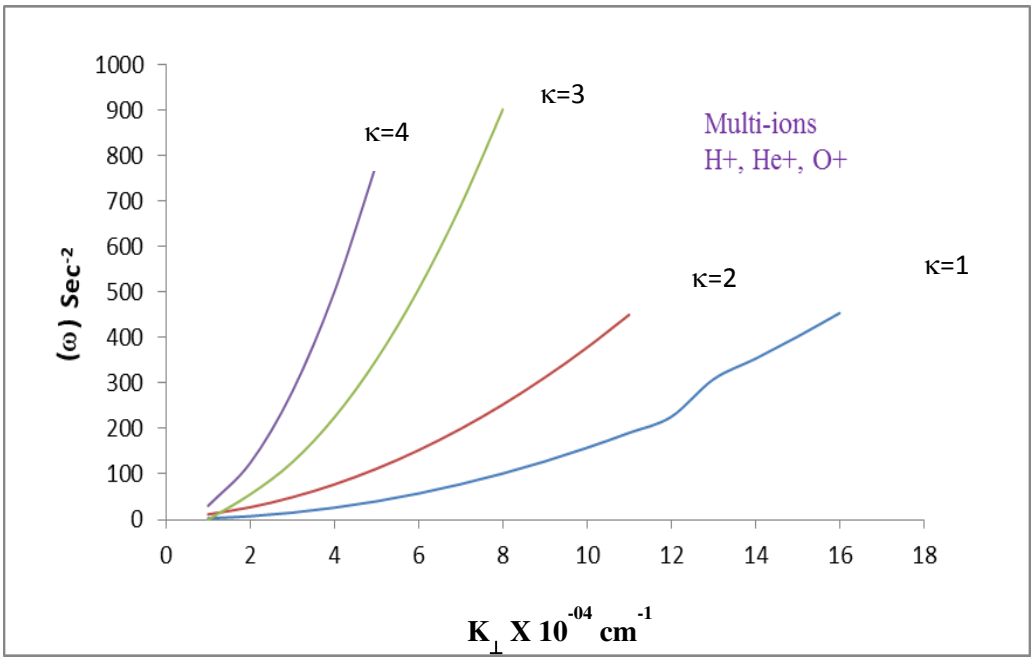

Figure 1: Shows the variation of wave frequency (ω) sec^{-2} versus wave vector $k_\perp$ (cm^{-1}) for different values of kappa distribution k = 1, 2, 3, 4.

Figure 1 shows the variation of the frequency of wave (ω) in sec^{-2} versus wave vector ($K_\perp$) in cm^{-1} for different values of kappa distribution k = 1, 2, 3, 4 for multi-ions magnetospheric plasma. It is found that expressions for dispersion relation are evaluated and results are presented in figure. Figure 1 shows the relation between the wave frequencies ω (sec^{-2}) versus wave vector $k_\perp$ (cm^{-1}). It is seen that wave frequency exponentially increases with increases of wave vector. It is seen that if we change the value of kappa distribution function k, wave frequency varies with wave vector.

Figure 2 shows the variation of growth rate γ versus wave vector $k_\perp$ (cm^{-1}) for different values of kappa distribution k = 1, 2, 3, 4 respectively in multi – ions plasma. The decreasing values of kappa distribution function k shows the increasing growth rate at particular value of wave vector $k_\perp$ of multi – ions plasma. It is noticed that after that particular value of wave vector, growth rate is linear. Which implies that growth rate increases at minimum value of kappa distribution function. The peak of the growth rate is increases with decrease of kappa distribution function of the ions in presence of EIC waves.

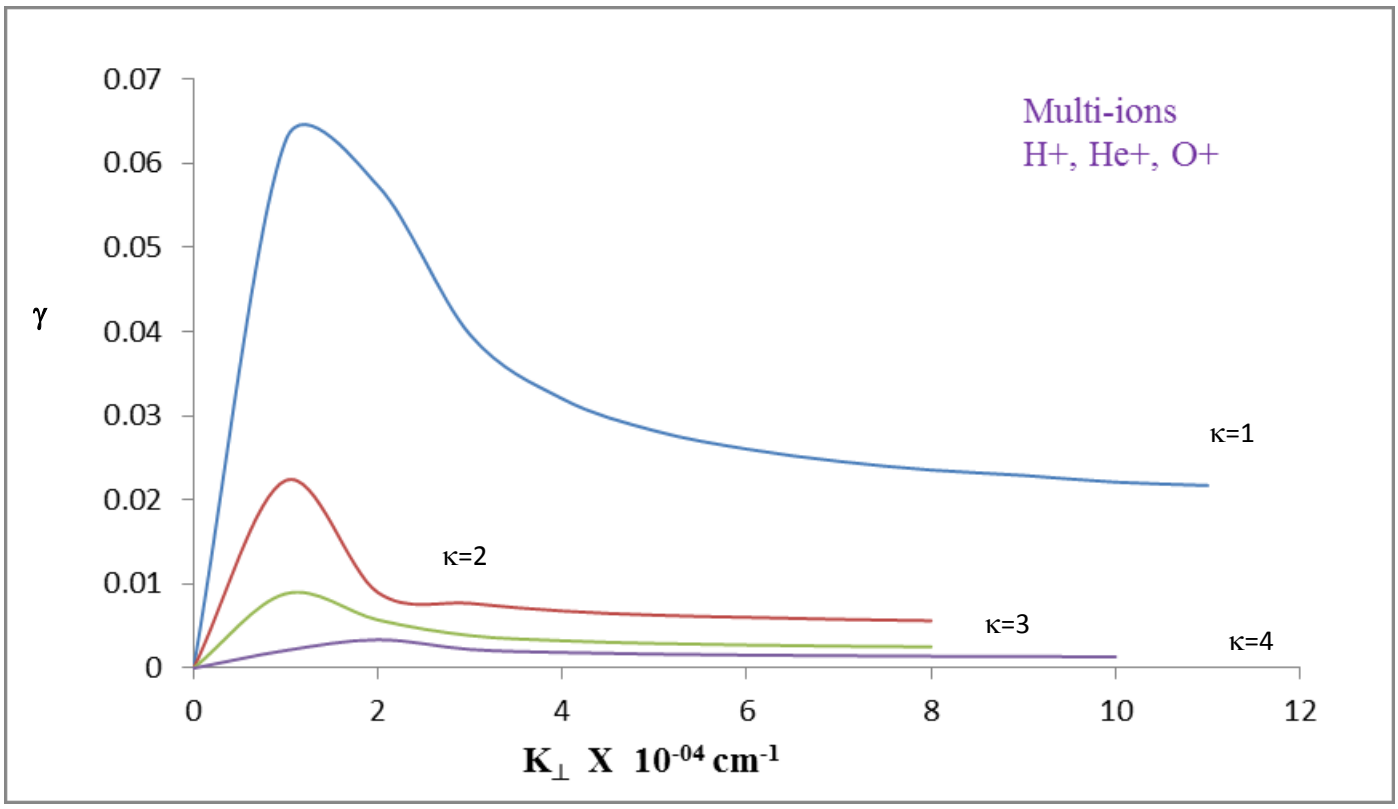

Figure 2: Shows the variation of growth rate γ versus wave vector $k_\perp$ (cm^{-1}) for different values of kappa distribution k = 1, 2, 3, 4.

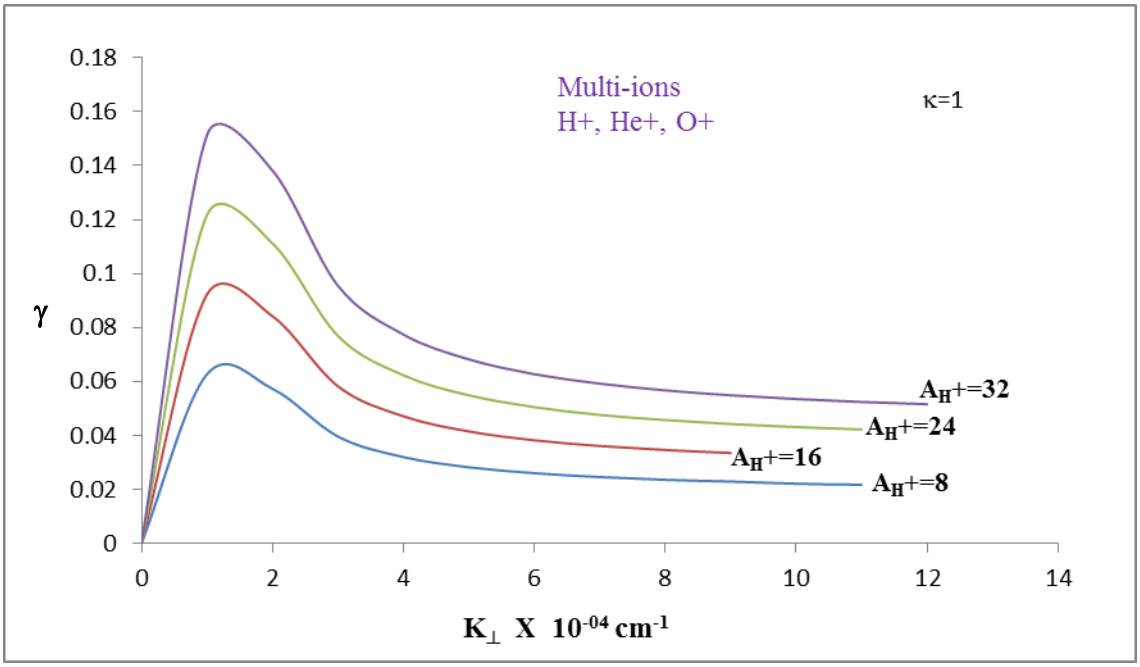

Figure 3: Shows the variation of growth rate γ versus wave vector $k_\perp$ (cm^{-1}) for different values of temperature anisotropy of hydrogen ions ($A_{H^+} = 8, 16, 24, 32$) for kappa distribution function k=1.

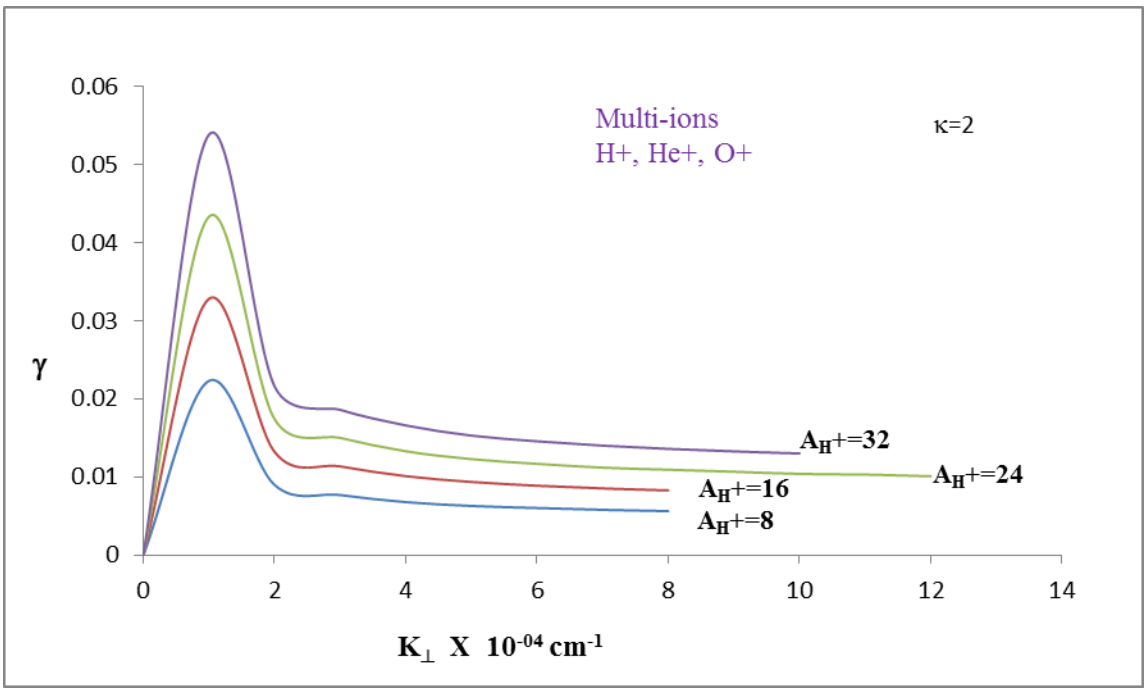

Figure 4: Shows the variation of growth rate γ versus wave vector $k_\perp$ (cm^{-1}) for different values of temperature anisotropy of hydrogen ions ($A_{H^+} = 8, 16, 24, 32$) for kappa distribution function k=2.

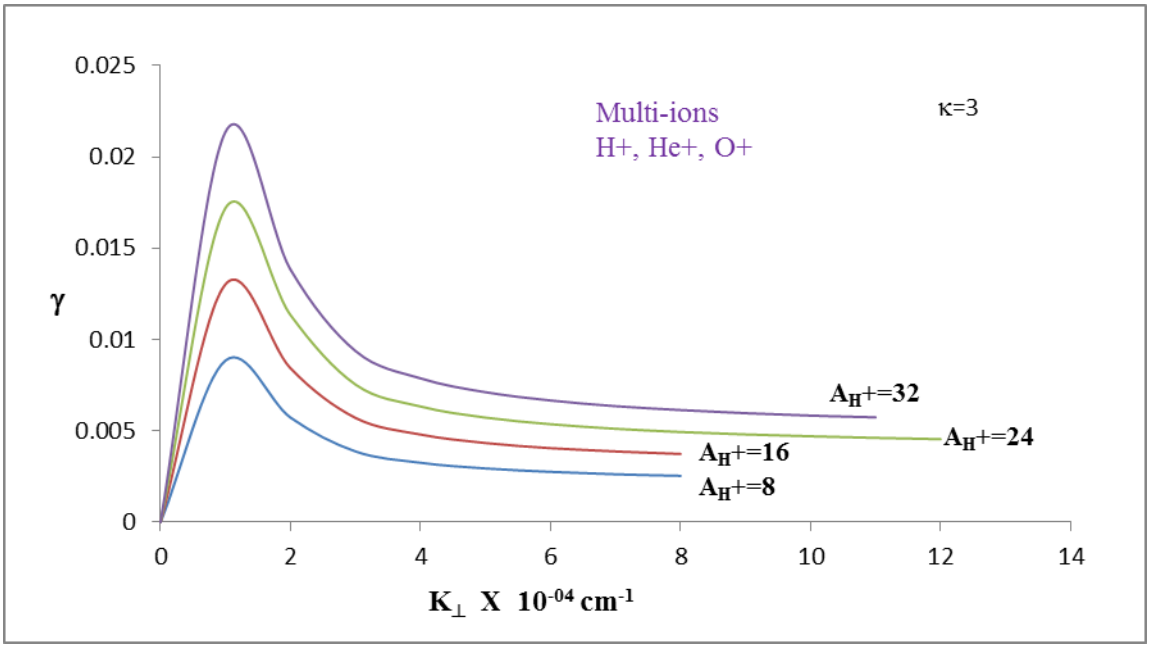

Figure 5: Shows the variation of growth rate γ versus wave vector $k_\perp$ (cm^{-1}) for different values of temperature anisotropy of hydrogen ions ($A_{H^+} = 8, 16, 24, 32$) for kappa distribution function k=3.

Figures 3, 4 and 5 shows the variation of growth rate γ versus wave vector $k_\perp$ for different values of temperature anisotropy of hydrogen ions ($A_{H^+} = 8, 16, 24, 32$) for kappa distribution function k = 1, 2, 3 respectively. Increase in value of A_{H^+}, has shown the increase in growth rate at particular value of wave vector $k_\perp$, after that growth rate goes linear corresponding temperature anisotropy with wave vector. The nature of growth rate is same for different values of temperature anisotropy of hydrogen. This may be due to more energetic particles may be available to provide energy to the wave by wave particle interaction due to landau damping and the wave will start to grow. Thus kappa distribution of magnetosphere can act as a free source of energy for wave generation.

Figures 6, 7 and 8 shows the variation of growth rate γ versus wave vector $k_\perp$ for different values of temperature anisotropy of helium ions ($A_{He^+} = 6, 12, 18, 24$) for kappa distribution function k = 1, 2, 3 respectively. Increase in value of A_{He^+}, has shown the increase in growth rate at particular value of wave vector $k_\perp$, after that growth rate goes linear corresponding temperature anisotropy with wave vector. This implies that the nature of growth rate is same for different values of temperature anisotropy of helium.

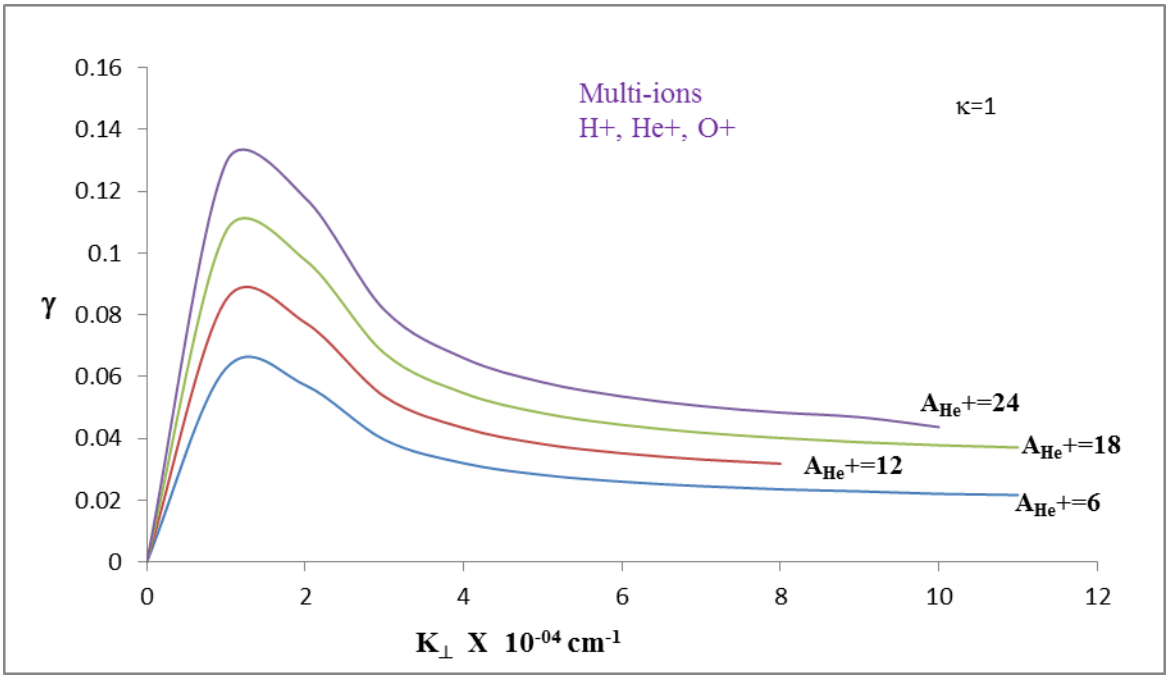

Figure 6: Shows the variation of growth rate γ versus wave vector $k_\perp$ (cm^{-1}) for different values of temperature anisotropy of helium ions ($A_{He^+} = 6, 12, 18, 24$) for kappa distribution function k=1.

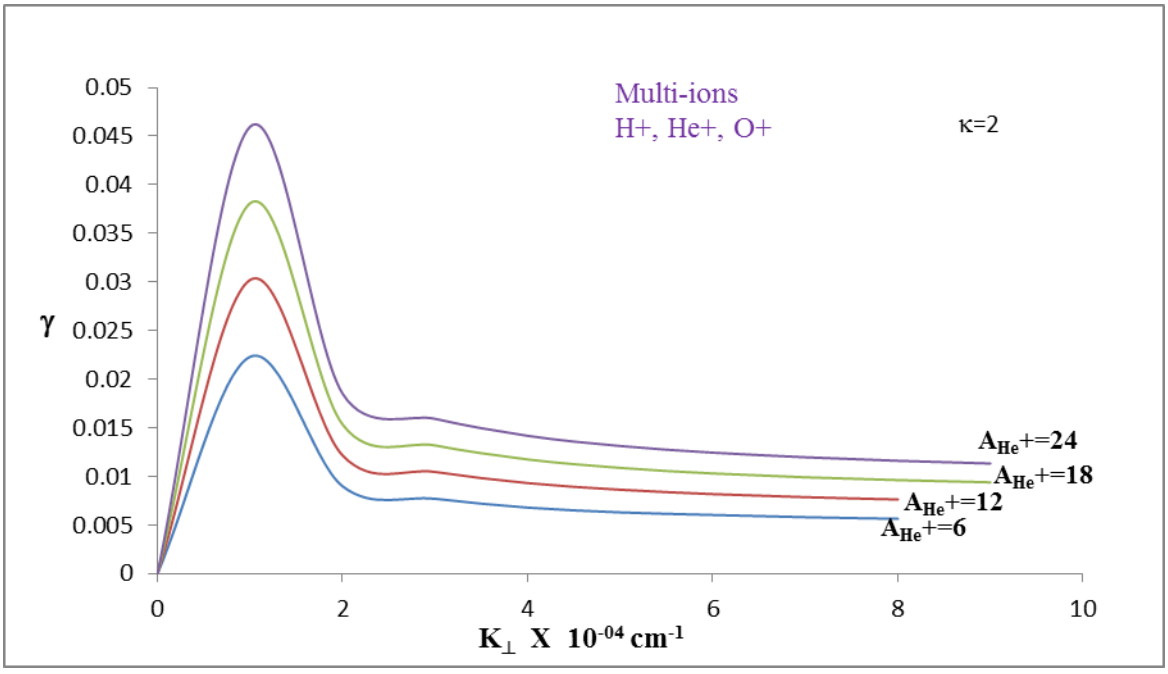

Figure 7: Shows the variation of growth rate γ versus wave vector $k_\perp$ (cm^{-1}) for different values of temperature anisotropy of helium ions ($A_{He^+} = 6, 12, 18, 24$) for kappa distribution function k=2.

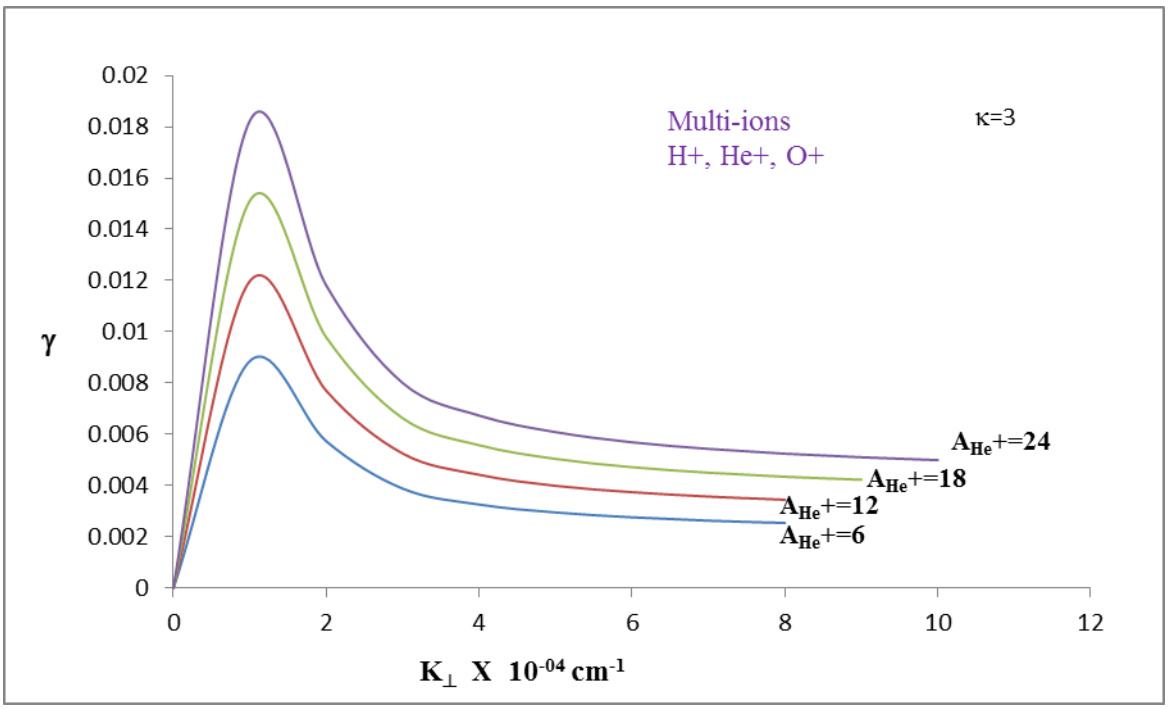

Figure 8: Shows the variation of growth rate γ versus wave vector $k_\perp$ (cm^{-1}) for different values of temperature anisotropy of helium ions ($A_{He^+} = 6, 12, 18, 24$) for kappa distribution function k=3.

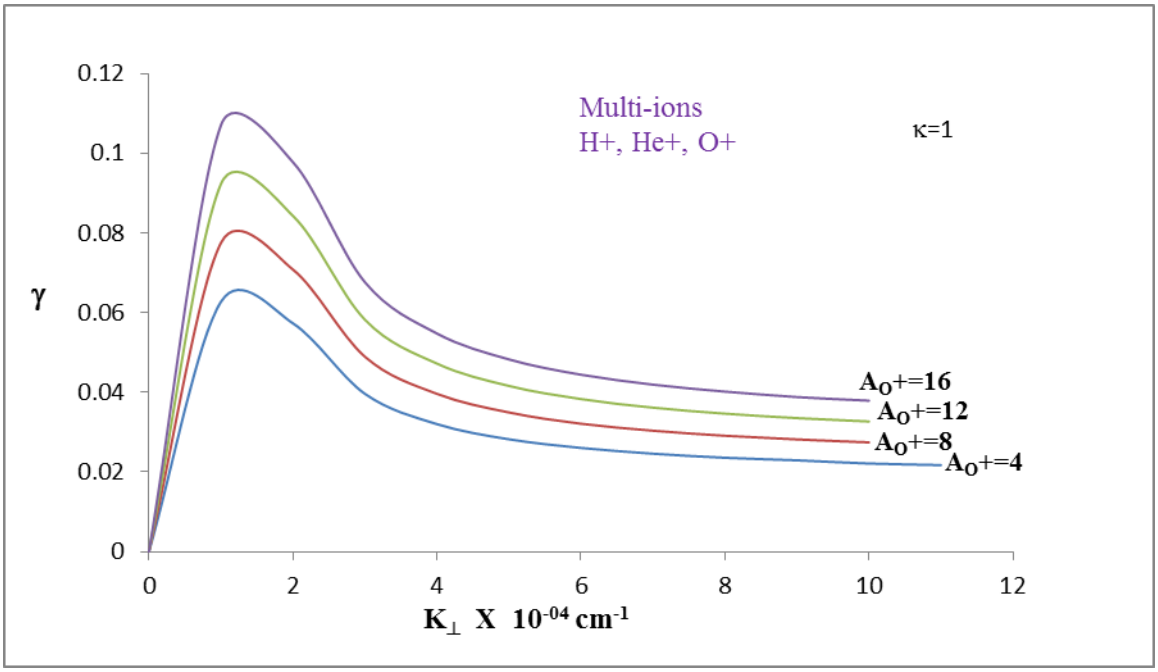

Figure 9: Shows the variation of growth rate γ versus wave vector $k_\perp$ (cm^{-1}) for different values of temperature anisotropy of oxygen ions ($A_{o^+} = 4, 8, 12, 16$) for kappa distribution function k=1.

Figures 9, 10 and 11 shows the variation of growth rate γ versus wave vector $k_\perp$ for different values of temperature anisotropy of oxygen ions ($A_{o^+} = 4, 8, 12, 16$) for kappa distribution function k = 1, 2, 3 respectively. Increase in value of A_{O^+}, has shown the increase in growth rate at particular value of wave vector $k_\perp$, after that growth rate get linear corresponding temperature anisotropy with wave vector. It means the nature of growth rate is same for different value of temperature anisotropy of oxygen.

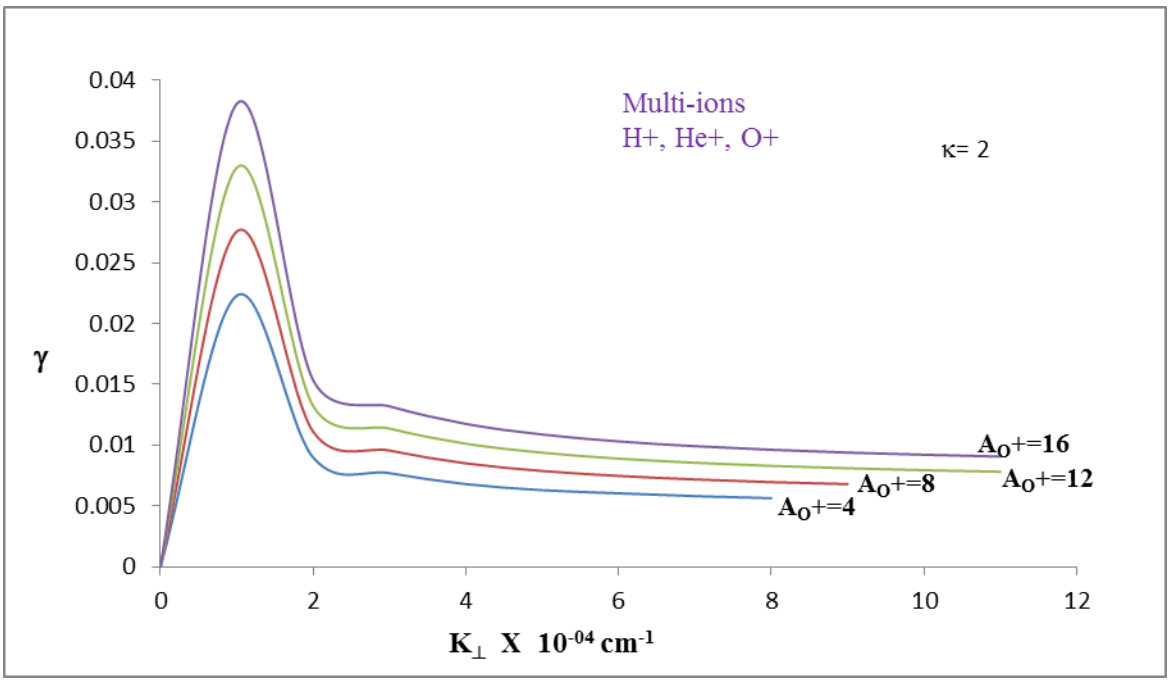

Figure 10: Shows the variation of growth rate γ versus wave vector $k_\perp$ (cm^{-1}) for different values of temperature anisotropy of oxygen ions ($A_{o^+} = 4, 8, 12, 16$) for kappa distribution function k=2.

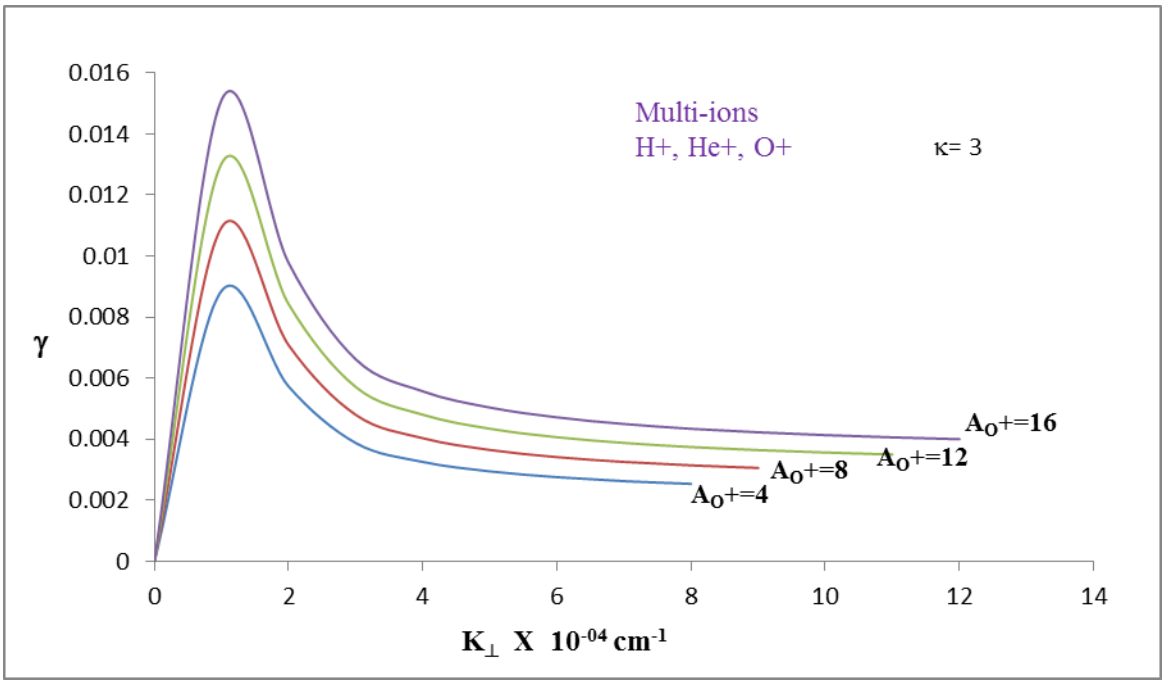

Figure 11: Shows the variation of growth rate γ versus wave vector $k_\perp$ (cm^{-1}) for different values of temperature anisotropy of oxygen ($A_{o^+} = 4, 8, 12, 16$) for kappa distributionfunction k=3.

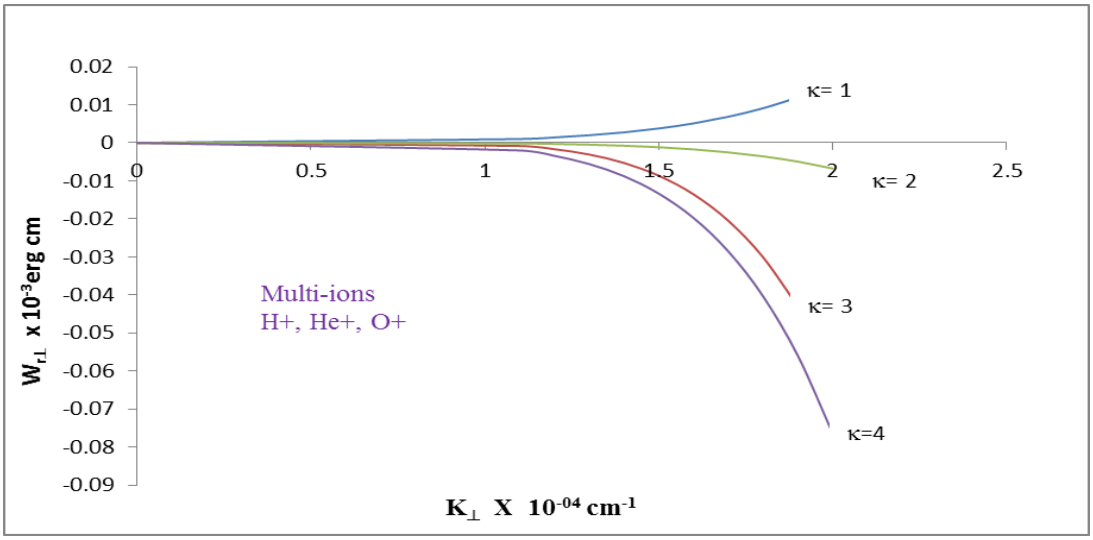

Figure 12: Shows Variation of perpendicular resonant energy $W_{r\perp}$(erg cm) versus perpendicular wave vector $K_\perp$ (cm^{-1}) for different values of kappa distribution function (k=1, 2, 3 and 4).

Figure 12 shows the variation of $W_{r\perp}$ versus $K_\perp$for different values of kappa distribution function k = 1, 2, 3 and 4. It is noticed that initially perpendicular resonant energy is zero for particular value of wave vector for the value of k respectively after that for the value of k=1, perpendicular resonant energy slightly increases with wave vector and for the value of k=2, 3, and 4 perpendicular resonant energy decreases with wave vector. This implies that perpendicular heating of resonant ions slightly increases at minimum value of kappa distribution function. As we increase the value of distribution function, resonant ions decrease.

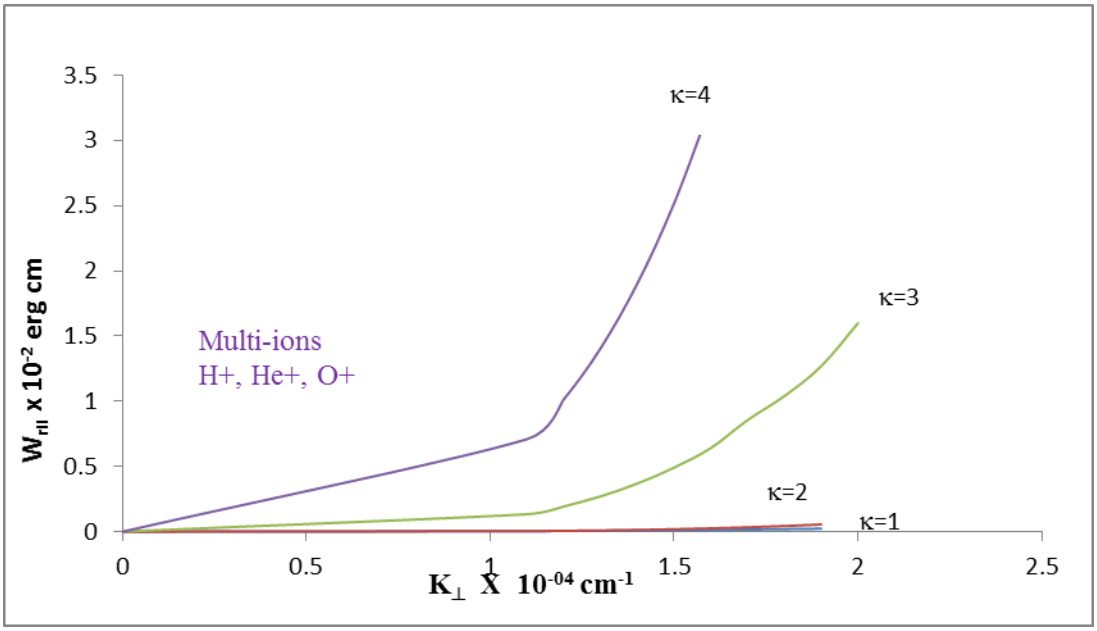

Figure 13: Shows Variation of parallel resonant energy $W_{r\parallel}$(erg cm) with perpendicular wave vector $K_\perp$ (cm^{-1}) for different values of kappa distribution function (k=1, 2, 3 and 4).

Figure 13 shows the variation of $W_{r\parallel}$ versus $K_\perp$for different values of kappa distribution k = 1, 2, 3 and 4. It is noticed that for the value of k=1, 2 parallel resonant energy is zero corresponding with wave vector after that for the value of k=1, parallel resonant energy slightly increases with wave vector and for the value of k=3, 4 parallel resonant energy initially linearly increases for particular value of wave vector after that parallel resonant energy exponentially increases. This implies that as we increase the value of kappa distribution function, parallel heating of resonant ions increases.

Conclusion

In this paper, we have studied effect of kappa distribution function on electrostatic ion cyclotron waves in multi-ions (H^+, He^+, O^+) magnetospheric plasma by particle aspect approaches. The ending comments of this study are as per monitors:

- We have obtained that increase in wave vector results exponentially increase in wave frequency.
- We found that the growth rate is higher for lower value of kappa at initial values of wave vector. Along with higher scale of wave vectors growth rate are becoming linear for all values of kappa.
- We have observed that growth rate is higher for higher value of temperature anisotropy of hydrogen, helium and oxygen at initial value of wave vector. On further scale of wave vector growth rate is becoming liner for all values of temperature anisotropy. Subsequently we found growth rate is higher for temperature anisotropy of hydrogen, helium and oxygen with lower value of kappa.
- Perpendicular resonant energy with respect to initial values of wave vector for different values of kappa is zero, on higher scale of wave vector we found only for lower value of kappa goes in positive direction and for all higher values of kappa this goes to negative direction.
- Parallel resonant energy with respect to wave vector is linear for lower value of kappa, increased value of kappa shows the exponential increasing conduct of parallel resonant energy.

The significance of this work may be importance in the electrostatic emission in the auroral acceleration region. The result of the study is also applicable to the plasma devices that have kappa distribution.

References

1. Drummond W.E. and Rosenbluth M.N. (1962) Anomalous diffusion arising from micro-instabilities in a Plasma‖ J Phys. Fluids, 5: 1507.
2. V.M. Vasyliunas (1968) A survey of low-energy electrons in the evening sector of the magnetosphere with Ogo 1 and Ogo 3. J. Geophys. Res. 73: 2839.
3. D.J. Williams, D.G. Mitchell and S.P. Christon (1988) Implications of large flow velocity signatures in nearly isotropic ion distributions. Geophys. Res. Let., lS, 303.
4. B. Abraham Schrauner, J.R. Asbridge, Bame and W.C. Feldman (1979) Proton- driven electromagnetic instabilities in high-speed solar wind streams. J. Geophys Res. 84: 553.
5. S.R. Church and R.M. Thorne (1983) On the origin of plasma sphere hiss: Ray path integrated amplification. J. Geophys. Res. 88: 7491.
6. M.P. Leubner (1982) On Jupiter's whistler emission. J. Geophys. Res. 87: 469.
7. T.P. Armstrong and T.H. Collison (1981) Voyager Observations of Possible Ion Acceleration near Ganymede. Spring AGU Meeting, May 1981, EOS, 62: 374.
8. S. P. Gary (1991) Electromagnetic ion instabilities and their consequences in space plasma. Space Sci. Rev. 56: 373.
9. L. Gomberoff and R. Elgueta (1991) Resonant acceleration of alpha particles by ion cyclotron waves in the solar wind. J. Geophys. Res. 96: 9801.
10. G. Gnavi, L. Gomberoff, F.T. Gratton, and R.M.O. Galvao (1996b) Electromagnetic ion-beam instabilities in cold plasma. J. Plasma Phys. 55: 77.
11. L. Gomberoff, and H.F. Astudillo (1998) Electromagnetic ion-beam plasma instabilities. Planet, Space Sci. 46: 1683.
12. G. Ahirwar, P. Varma, and M.S. Tiwari (2010) Study of electromagnetic ion- cyclotron waves with general loss-cone distribution and multi-ions plasma-particle aspect approach. Ind. J. of Pure& Appl. Phys. 48: 334.
13. Escoubet, C.P., Schmidt R. and Goldstein M.L. (1997) Cluster Science and mission overview‖. Space Sci. Rev., 79: 11–32.
14. Nishida, A. (1994) The GEOTAIL mission. Geophys. Res. Lett., 21: 2871-2873, Doi: 10.1029/94GL01223.

15. Liu, Z.X., Escoubet, C.P., Pu, Z., Laakso, H., Shi, J.K., Shen, C. and Hapgood, M. (2005) The Double Star mission‖ Ann. Geophys., 23: 2707–2712, Doi: 10.5194/angeo-23-2707-2005.
16. Angelopoulos, V. (2008) The THEMIS Mission‖, Space Sci. Rev., 141: 5–34, Doi: 10.1007/s11214-008-9336-1.
17. Mishra, R and MS Tiwari (2006) Effect of parallel electric field on electrostatic ion cyclotron instability in anisotropic plasma in the presence of ion beam and general distribution function. Planet. Space Sci., 54: 188.
18. Tiwari, MS and Rostoker, G (1984) Field aligned currents and auroral acceleration by non-linear MHD waves. Planet. Space Sci., 32: 1497–1503.
19. Mozer FS, Ergun R, Temrin M, Cattell C, Donsbeeck J & Wygant J, Phys Rev Lett, 79 (1997) 1281.
20. Duan S.P., Li, Z.Y., and Liu, Z.X (2005) Kinetic Alfv´en wave driven by the density in homogeneity in the presence of loss-cone distribution function-Particle aspect analysis. Planet. Space Sci., 53: 1167–1173.